Iranian Journal of Chemical Engineering
Vol. 1, No. 2, summer & autumn 2004, IACHE

Newtonian and Non-Newtonian Blood Flow Simulation after Arterial Stenosis- Steady State and Pulsatile Approaches

M. Moshkelani, S. Gh. Etemad[*]*, and A. Moheb*
Chemical Eng. Dept., Isfahan University of Technology, Isfahan 84155, IRAN

Abstract
Arterial stenosis, for example Atherosclerosis, is one of the most serious forms of arterial disease in the formation of which hemodynamic factors play a significant role. In the present study, a 3-D rigid carotid artery with axisymmetric stenosis with 75% reduction in cross-sectional area is considered. Laminar blood flow is assumed to have both Newtonian and non-Newtonian behavior (generalized Newtonian fluid), while steady state and pulsatile cases are imposed separately. Governing equations are momentum and continuity. Employing the finite volume technique, flow features such as velocity profiles, flow separation zone and wall shear stress distribution in post stenotic region are calculated. Based on the results of the steady state situation, reverse and circulating flows exist until far from stenosis in Newtonian case. But, in non-Newtonian condition, these regions are limited to smaller areas near the stenosis. As blood flow becomes unsteady, in Newtonian case reverse flows become larger and stronger even far from stenosis while circulating flows weaken. Considering the same assumptions with non-Newtonian behavior, circulating flows become stronger than those of Newtonian model, while reverse flows weaken. Obtained results agree with the analytical results available for Newtonian fluid..

Keywords: *Numerical Simulations, Flow Separation, Wall Shear Stress, Stenosis, Power Law*

Introduction
Stenosis means reduction in the cross-sectional area of blood vessels. When it happens in large or medium sized arteries, it will cause Atherosclerosis. This problem occurs when lipid and cholesterol as well as proliferation of connective tissues cause stenosis. This area reduction alters the normal hemodynamic conditions for further influence on disease development [1,2]. For instance, wall shear stress directly affects biological function of tissues, so that shear stress fluctuation causes plaque rupture that leads to aggregation of stenosis degree and thrombosis.

The first study on stenosis is referred to Mann *et al.* in 1938. All attempts in this field so far can be categorized into experimental, analytical and numerical methods. *In vivo* experiments show that hemodynamics has a very special effect on atherosclerosis [3-5] and also results obtained from rotating viscometer describe the relationship between hematocrit and non-Newtonian blood flow behavior [6,7]. Many other studies illustrated that under low shear rate blood behaves as

∗- Corresponding author: Tel: +98-311-3915625, fax: +98-311-3912677, E-mail address: etemad@cc.iut.ac.ir

non-Newtonian fluid characterized by Casson model [8]. Besides, other experiments using Laser Doppler anemometry [9] and hydrogen bubble and dye injection methods [10-12] have yielded some significant results on wall shear stress.

Most of the investigations in this field were based on steady state Newtonian blood flow for mild stenosis [13-15]. For example, by solving steady state blood flow features through axisymmetric stenosis, Smith [16] calculated the flow parameters in post stenotic region and indicated high dependency of these parameters on entrance Reynolds number and stenosis geometry.

Using the finite difference method, Deshpande [17] solved steady state Newtonian laminar blood flow through stenosis. Many other researchers simulated the problem using pulsatile or non-Newtonian model [18-23]. The main purpose of this paper is to simulate post stenotic flow at physiologically realistic flow conditions in axisymmetrical stenosed Carotid artery with 75% reduction in cross sectional area. Blood flow is assumed to be Newtonian and power law model non-Newtonian and the domain is 3-D with a rigid wall.

Method

Stenosis Geometry

Among of all the different stenosis shapes presented in the literature, in this study the one shown in Figure 1 is considered to have the proper geometry. A total of 30 carotid arteries (a carotid artery is an artery that transfers blood to upper parts of body through neck) have been examined by using an ultrasound scanner and some images were acquired [24]. Stenosis happens more likely in bend shaped vessels but since the location of stenosis in this article is obtained experimentally and mathematically [24], the stenosis geometry is not a far-fetched assumption. As shown in Figure 1, stenosis comprises two sections of diameter change on both sides and a flat region in between. The inlet diameter is 8mm, pre and post stenosis lengths are 48mm and 180mm, respectively, and also whole stenosis length is 16.07mm. Proximal and distal ends are each approximated with an error function with a length of 4.7mm. Because of the symmetry assumed in the artery, one quarter of it was considered as flow domain. In this investigation, the vessel walls are elastic, but rigid artery walls is taken as a simplifying assumption in this study.

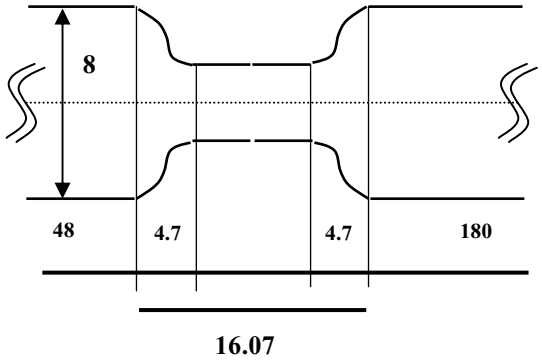

Figure 1. Stenosis geometry

Governing Equations and Boundary Conditions

The governing equations are continuity (Eq. 1) and momentum equations (Eq. 2) where power law model is used as the constitutive equation (Eq. 3).

$$\frac{\partial \rho}{\partial t} + \nabla \cdot (\rho u) = o \qquad (1)$$

$$\rho \frac{Du}{Dt} = \nabla \cdot \sigma \quad \sigma_{ij} = -p\delta_{ij} + \tau_{ij} \qquad (2)$$

$$\tau = \mathrm{K}(\dot{\gamma})^{\mathrm{n}} \qquad (3)$$

while ρ, t, u, σ, τ, K, $\dot{\gamma}$ and n represent density, time, velocity vector, stress tensor, shear stress tensor, consistency index, shear rate tensor and power law index, respectively.

These equations are solved employing the finite control volume technique. A non-uniform mesh distribution with 30000 elements was considered, which is finer at wall regions. Equations were fully implicit in

time and second upwind differencing was employed for all equations. Mesh generation is done using Gambit software and simulation is carried out using Fluent software.

No-slip conditions on walls and fully-developed conditions at the outlet plane, and two symmetry conditions (due to axisymmetric stenosis) are assumed as boundary conditions. In the steady state case, the entrance Reynolds number is 672. The maximum value at systole peak is chosen because blood velocity reaches its maximum value at this point and makes a critical condition. In the pulsatile case, the variation of inlet velocity is shown in Figure 2 in different systole and diastole time steps (t_p is called heart pulse period, which is equal to 0.8 sec). In the pulsatile case, the effects of one pulse on blood flow features are presented. Blood density (in both Newtonian and non-Newtonian cases) and viscosity (in Newtonian model) are 1035kg/m^3 and 0.00414 kg/ms, respectively. In power law model, consistency index is 0.1293 kg/ms^{2-n} and power law index is 0.35.

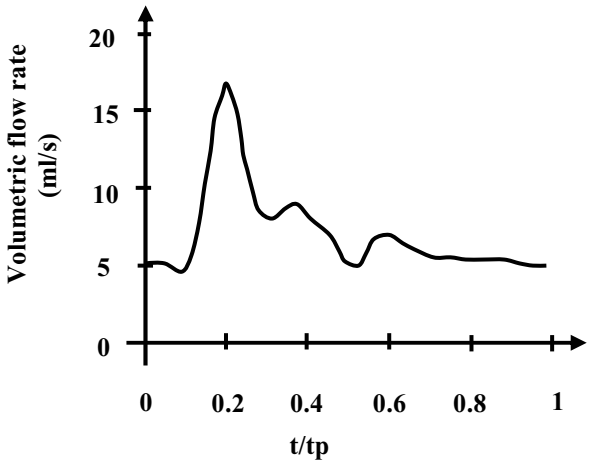

Figure 2. Human carotid artery waveform

Results

Since the results in this article are based on numerical simulation, it is useful to compare results obtained under simple conditions with available analytical results. The relationship between friction factor and Reynolds number in Newtonian case is as follows:

$$f.Re = 16 \quad (4)$$

where f and Re are Fanning friction factor and Reynolds number, respectively. For fully developed flow, Newtonian fluid, and steady state conditions in the case of 75% area reduction, the product of friction factor and Reynolds number was 16.101, which is very close to the analytical results (Eq. 4). Also, the velocity profile for n=1 was in excellent agreement with the profile obtained from the analytical solution.

Generally, blood velocity increases when entering stenosis, and as a result, blood pressure decreases. Therefore, the velocity reaches its maximum value in passing through the stenosis throat. When blood leaves stenosis, because of sudden expansion the velocity decreases gradually. So, boundary layer separation happens near artery walls. Consequently, wall shear stress becomes zero and reverse flow occurs. Also, vortices become inevitable. As blood moves forward, flow parameters recover to some extent, depending on the blood behavior and the model employed. For example, in non-Newtonian case, blood inlet conditions are obtained farther from stenosis (in downstream region) compared to the Newtonian case. So, dominant secondary flows are seen until blood becomes fully developed in downstream region. For better understanding of flow features, the region downstream of stenosis is divided into different sub regions separated by planes 1D, 3D, 6D, 9D, 12D and 15D, where D is the vessel diameter and the numbers denote the distance by which the plane is away from the stenosis. For instance, 3D is a plane three diameters downstream of the stenosis.

Steady-State Blood Flow

Newtonian Model

In this case, flow separation zones and reverse flows are strong and dominant as they exist even at 9D and also there are circulating flows even at 12D. Wall shear stress reaches

zero immediately after leaving stenosis and then becomes negative until 0.13 meter of artery length and after that it becomes positive. Figure 3 shows wall shear stress distribution and the flow separation zone. The velocity profile at plane 1D is presented in Figure 4. From this figure, the maximum velocity value corresponds to the artery symmetry line. Also reverse velocity vectors exist near walls occupying a large radial area of the artery. Figures 5 and 6 show vortices near and far from stenosis (at 1D and 9D), respectively.

Non-Newtonian Model

In the non-Newtonian model, flow separation zones are weaker compared to the Newtonian case as they exist only up to 3D and do not spread vastly like in the Newtonian model. Wall shear stress, velocity profile and circulating flows are demonstrated in Figures 7, 8, 9 and 10, respectively. Wall shear stress value changes until it reaches zero after stenosis and then becomes negative in 0.08m of artery length (Figure 7). From Figure 8, it is clear that reverse flows are limited to a very thin layer. According to Figures 9 and 10, circulating flows remain until 9D, which are again formed in more limited area. All other disturbances, which remain longer in non-Newtonian model, are due to secondary flows.

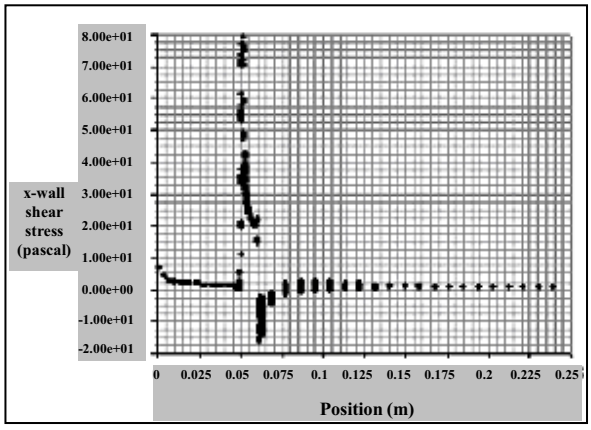

Figure 3. Wall shear stress, Newtonian, steady state

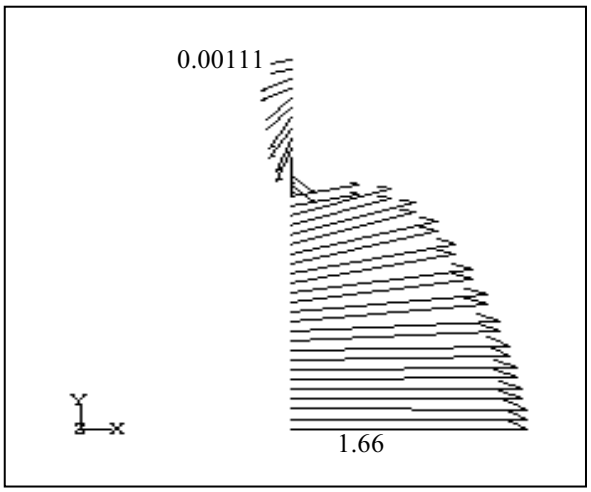

Figure 4. Velocity profile, Newtonian, steady state, plane 1D

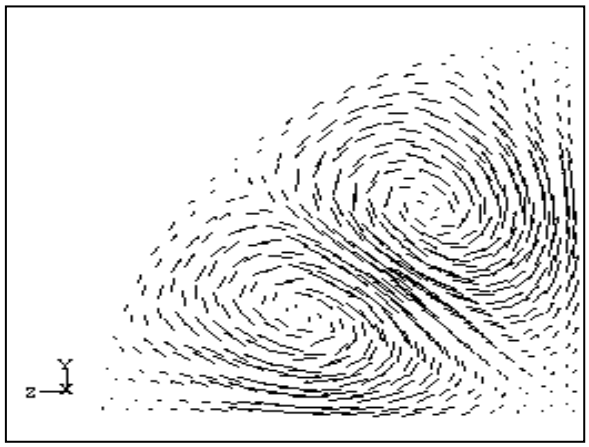

Figure 5. 2-D velocity vector, Newtonian, steady state, plane 1D

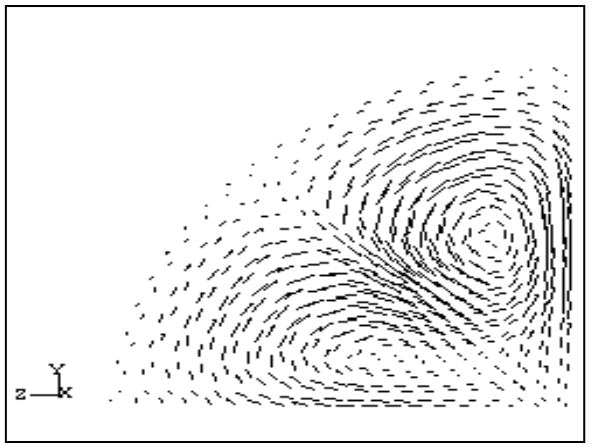

Figure 6. 2-D velocity vector, Newtonian, steady state, plane 9D

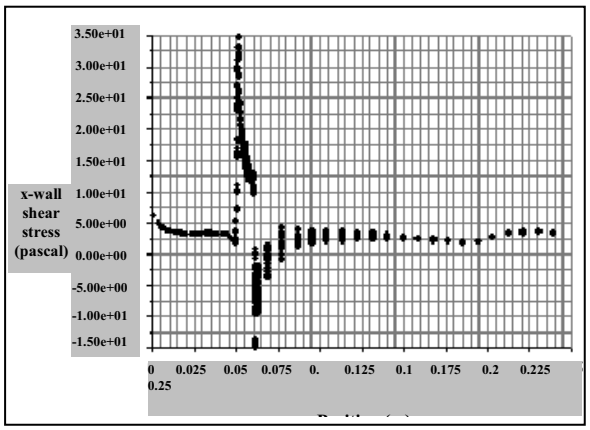

Figure 7. Wall shear stress, non-Newtonian, steady state

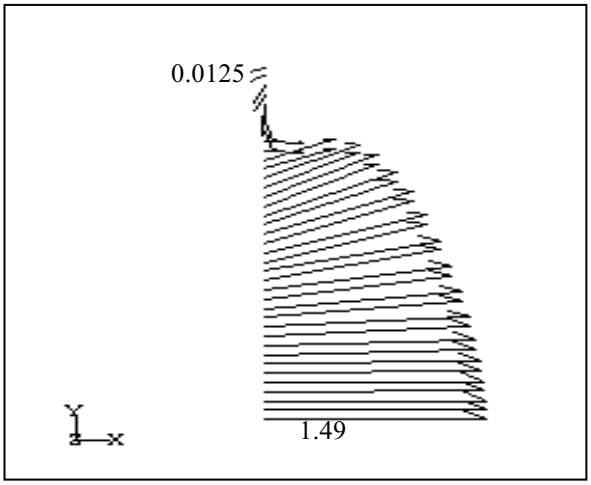

Figure 8. Velocity profile, non-Newtonian, steady state, plane 1D

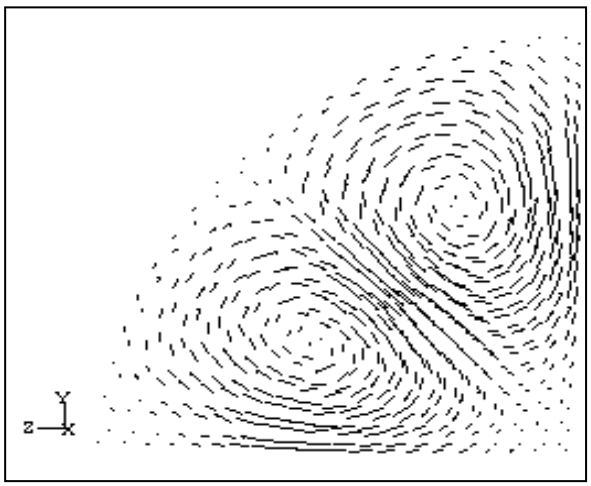

Figure 9. 2-D velocity vector, non-Newtonian, steady state, plane 1D

Pulsatile Blood Flow

Newtonian Model

Figure 11 presents the wall shear stress for systole peak, pulsatile flow and Newtonian model while velocity vector and contour plots are demonstrated through figures 12-15. In the early part of systole from t/tp=0 to 0.08 blood flow decelerates. Thus, flow separation zone and reverse flow occur until 6D. In this stage, no significant vortex is seen. Between t/tp=0.08 to 0.2, blood flow accelerates and at 0.2 it reaches a systole peak. So, reverse flows happen even at 15D in post stenotic region, but fully-developed conditions are obtained at outlet. Also, small vortices are perceived at plane 1D. Blood flow velocity decreases untill t/tp= 0.32.

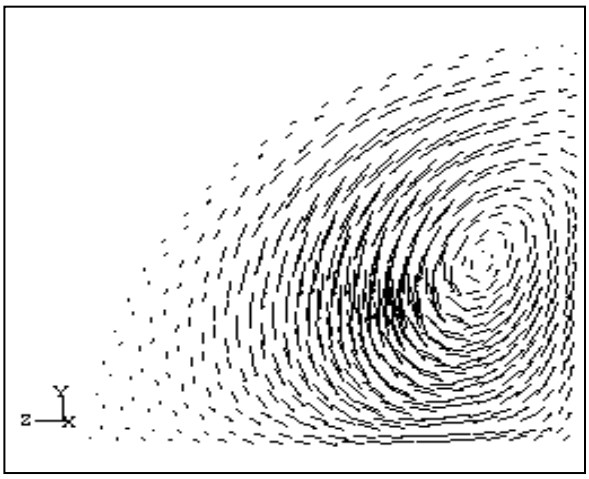

Figure 10. 2-D velocity vector, non-Newtonian, steady state, plane 9D

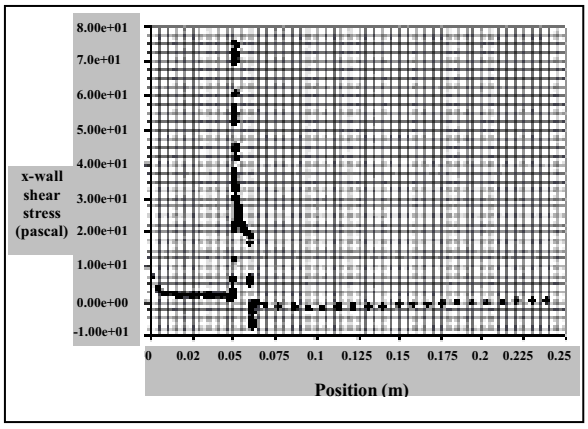

Figure 11. Wall shear stress, Newtonian, systole peak, pulsatile

Therefore, reverse flow doesn't exist after 9D, but vortices become larger so at 6D they exist, and they appear to be pushed toward the line of symmetry. From t/tp= 0.32 to 0.36, reverse flows exist until 9D. The last stage from t/tp=0.4 to 0.52, where flow completely decelerates and blood flow pattern weakens and at t/tp=0.52, there is not a reverse flow at 3D, and circulating flows become weak even at 1D, and vortex moves to the symmetry line. Wall shear stress reaches its maximum value at t/tp=0.2 (at systole peak).

Non-Newtonian Model

Figure 16-20 present the wall shear stress, velocity vector and contour plots for systole peak, pulsatile flow and non-Newtonian model.

From t/tp=0 to 0.08, when blood flow decelerates, reverse flow is not seen in post stenotic region, but circulating flows increase when velocity decreases. When blood flow accelerates and reaches the maximum peak value in systole (t/tp = 0.2), reverse flows exist even after 3D. Circulating velocity vectors are seen in a wide region in plane 1D near wall. This is true up to 6D. At this plane, no reverse flows occur but immediately after that, between plane 9D up to 15D, disturbance in velocity vectors are seen. As velocity decreases reverse flows discourage but circulating core (t/tp=0.2 to 0.32), reverse flows weaken; of course, at 0.24 there is a flow separation zone at 1D. Totally in decelerating phase in one time step as blood goes away from stenosis, vortex moves away from symmetry line to the other symmetry face, which does not contain symmetry line. In the second velocity increasing phase (t/tp= 0.32 to 0.36), beings at symmetry face (which does not contain symmetry line). In the second decelerating phase from t/tp= 0.4 to 0.54, reverse flow is seen at plane 1D and as velocity decreases, reverse flow and vortices weaken. But, flow disturbance is seen even far from stenosis and at out flow velocity vectors are inclined to the symmetry face and wall corner.

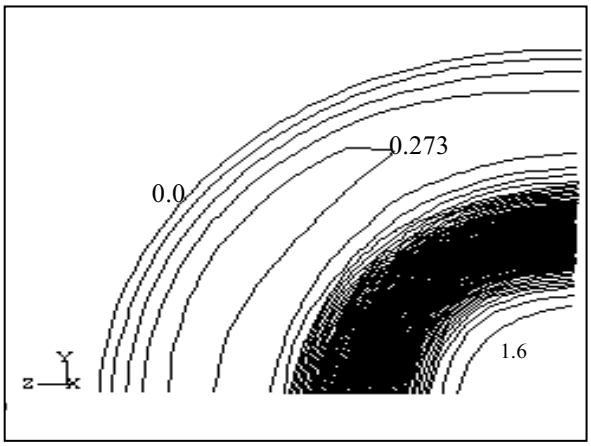

Figure 12. Velocity contours, Newtonian, plane 1D, systole peak, pulsatile

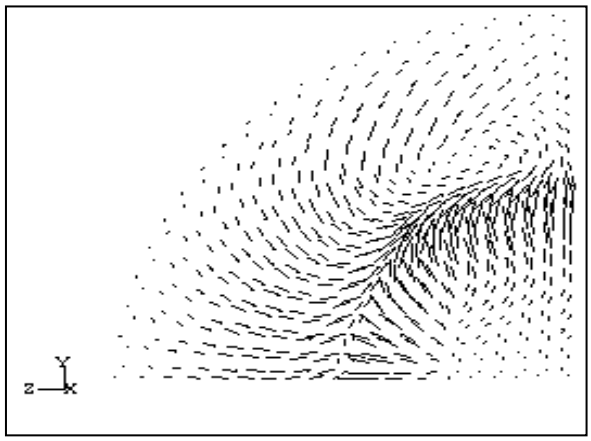

Figure 13. 2-D velocity vector, Newtonian,plane 1D, systole peak, pulsatile

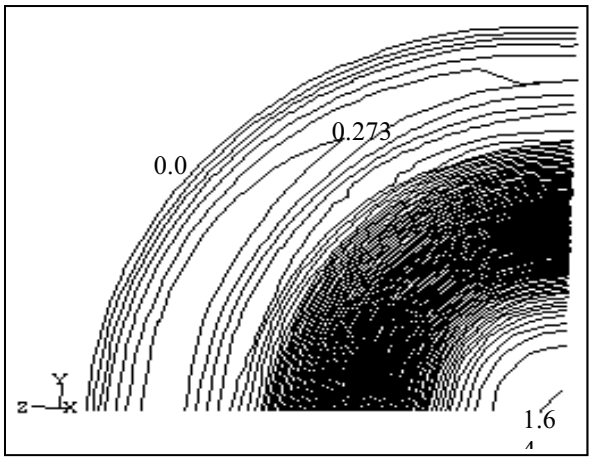

Figure 14. Velocity contours Newtonian, plane 3D, systole peak, pulsatile

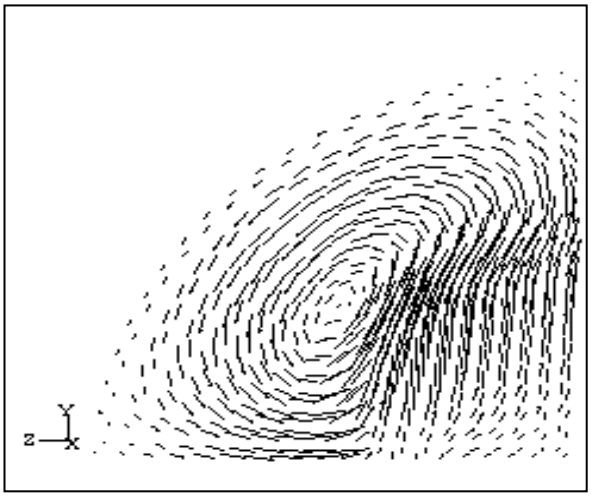

Figure 15. 2-D velocity vector, Newtonian, plane 1D, t/t_p=0.32

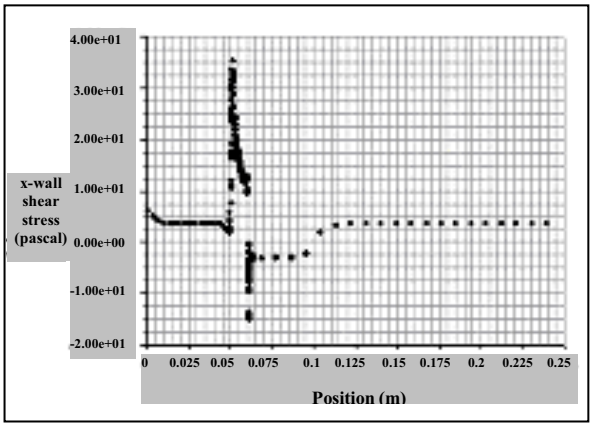

Figure 16. Wall shear stress, non-Newtonian, systole peak, t/t_p=0.32

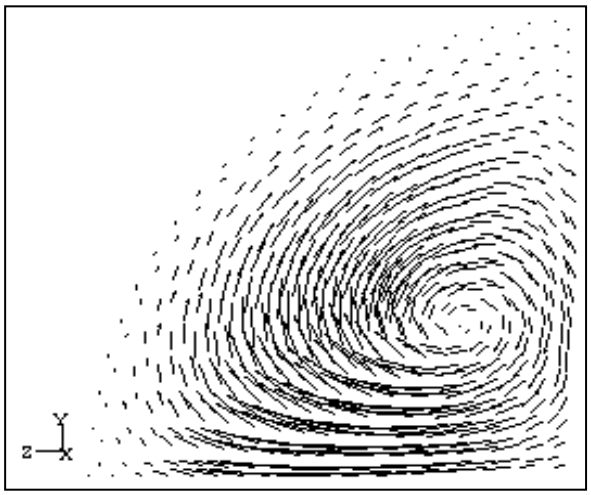

Figure 17. 2-D velocity vector, non-Newtonian, plane 1D, t/t_p=.08

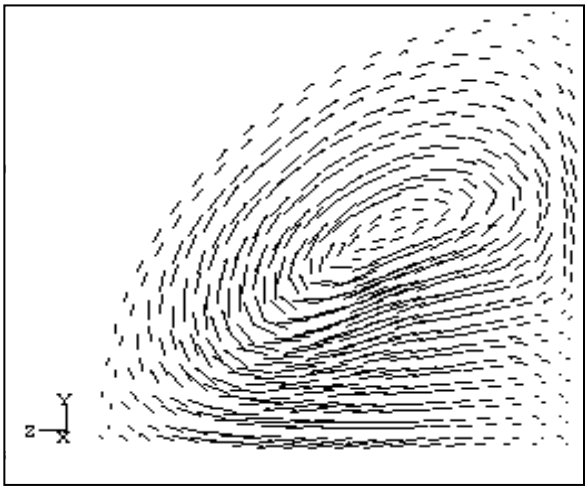

Figure 18. 2-D velocity vector, non- Newtonian, plane1D, t/t_p=0.2

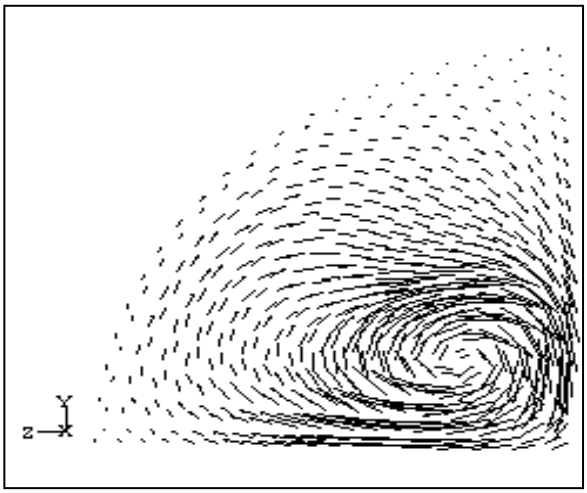

Figure 19. 2-D velocity vector, non Newtonian, plane 1D, t/t_p=0

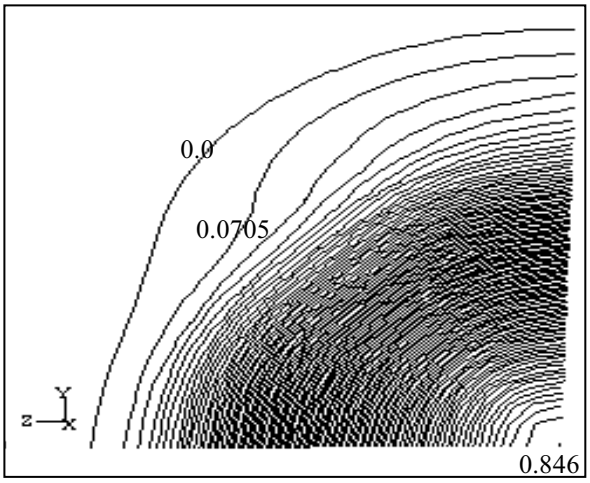

Figure 20. Velocity contour, non-Newtonian, plane 3D, t/t_p=0.32

Conclusions

In this investigation, blood flow features along stenosis were considered. In steady state and Newtonian blood flow, reverse and circulating flows are stronger than in the non-Newtonian case and they exist farther from stenosis compared to the non-Newtonian one. Maximum shear stress reaches its greatest value for Newtonian fluids among all models, but secondary flows exist longer in the non-Newtonian case. In pulsatile model and in the Newtonian case, reverse flow exists even far from stenosis, but it becomes a limited region in the non-Newtonian case. Vortices exist in both models. As Reynolds number reaches 2000 (at systole peak and at stenosis throat), blood flow becomes turbulent. Non-Newtonian behavior enforces vortices and flow remains disturbed for a long time.

References

1. Tu, C., and Deville, M. "Pulsatile flow of non-Newtonian fluids through arterial stenosis", *Journal of Biomech*., 29, 899(1996).
2. Texon, M. "The role of vascular dynamics in the development of atherosclerosis", Academic Press, p. 167(1963).
3. May, A., Weese, J.A.G., and Rob, C.G., "Hemodynamic effect of arterial stenosis", *Journal of Surgery,* 53, 513(1963).
4. Fidd, R.V., Byar, D., and Edwards, E.A., "Factors affecting flow through a stenosed vessel", *Archives of surgery,* 88, 83(1964).
5. Kindt, G.W., and Aulian, R., "The effect of stricture length on critical arterial stenosis", *Surgery, Gynecology and Obstetrics*, 128, 729(1969).
6. Bugliarello, G., Kapur, C., and Hsiao, G., "The profile viscosity and other charactrestics of blood flow in a non-uniform shear field", Proceeding of *The Fourth Int. Cong. on Rheology 4 Symp. Of Biorheology,* pp. 351-370(1965).
7. Rand, P.W., Lacombe, E., and Austin, W.H., "Viscosity of normal blood under normothermic and hypothermic conditions", *J.appl.Physiol*., 19, 117(1964).
8. Merrill, F.W., Benis, A.M., and Salzman, E.W., "Pressure-flow relations of human blood in hollow fibers at low flow rates", *J. appl. Physio*., 20, 954(1965).
9. Ahmed, S.A., and Giddens, D.P., "Pulsatile poststenotic flow studies with laser Doppler anemometry", *J. Biomech.,* 17, 695(1984).
10. Lieber, B., "Order and random structures in pulsatile flow through constricted tubes", *Ph.D Thesis*, Georgia Ins. Tech, Atlanta (1985).
11. Ojha, M., and Cobbold, R.S.C., "Pulsatile flow through constricted tubes: an experimental investigation using photocromic tracer methods", *J. Fluid Mech.*, 203, 173(1989).
12. Gijsen, F.J.H., and Palmen, D.E.M., "Analysis of the axial flow fuild in stenosed caritid artery bifurcation models LDA experiments", *J. Biomech*, 11, 1483(1996).
13. Shukla, J.B., Parihar, R.S., and Gupta, S.P., "Effects of peripheral layer viscosity on blood flow through the artery with mild stenosis", *Bull. Math. Biol.,* 42, 797(1980).
14. Misra, J.C., Patra, M.K., and Misra, S.C., "A non-Newtonian fluid model for blood flow through arteries under stenotic conditions", *J.Biomech.,* 26, 1129(1993).
15. Damodaran, V., and Chang, C., "Numerical study of steady laminar flow through tubes with multiple constrictions using curvilinear co-ordinates", *J. Num.Meth. fluids,* 23, 1021(1996).
16. Smith, F.T., "The separation flow through a severely constricted symmetric tube", *J. Fluid Mech*., 90, 725(1979).
17. Deshpande, M.D., Giddens, D.P., and Mabon, R.F., "Steady laminar flow through modeled vascular stenoses", *J.Biomech.,* 9, 165(1976).
18. Fukushima, T., Azuma, T., and Matsuzawa, T., "Numerical analysis of blood flow in the vertebral artery", *J.Biomech.Eng.*, 104, 143(1982).
19. Theodorou, G., and Bellet, D., "Laminar flows of a non-Newtonian fluid in mild stenosis", *Computer methods in applied Mech. and Eng.,* 54, 111(!986).
20. Nakamura, M., and Sawada, T., "Numeric al study on the unsteady flow of Non-Newtonian fluid", *J. Biomech. Eng.,* 112, 100(1990).

21. Theodorou, G., and Bellet, B., "Laminar flows of a non-Newtonian fluid in mild stenosis", *Computer methods in applied Mech. and Eng*., 54, 111(1986).
22. Moayeri, M.S., and Vali, A., "Effects of non-Newtonian properties of blood on flow characteristics through a stenosis", *Iranian J. Science and Technology,* 20(1), 25(1996).
23. Deplano, E., and Siouffi, M., "Experimental and numerical study of pulsatile flows through stenosis: wall shear stress analysis", *J. Biomec*., 32, 1081(1999).
24. Long, Q., and Xu, X.Y., "Numerical investigation of physiologically realistic flow through arterial stenosis", J. Biomech., 34, 1229(2001).